Biochimica et Biophysica Acta 1838 (2014) 2078–2086

Contents lists available at ScienceDirect

Biochimica et Biophysica Acta

journal homepage: www.elsevier.com/locate/bbamem

Lipid binding specificity of bovine α-lactalbumin: A multidimensional approach

Arunima Chaudhuri, Amitabha Chattopadhyay *

CSIR-Centre for Cellular and Molecular Biology, Uppal Road, Hyderabad 500 007, India

ARTICLE INFO

Article history:
Received 12 January 2014
Received in revised form 27 April 2014
Accepted 28 April 2014
Available online 4 May 2014

Keywords:
Bovine α-lactalbumin
BLA tryptophan
Di-8-ANEPPS
REES
Lipid–protein interaction
Membrane penetration depth

ABSTRACT

Many soluble proteins are known to interact with membranes in partially disordered states, and the mechanism and relevance of such interactions in cellular processes are beginning to be understood. Bovine α-lactalbumin (BLA) represents an excellent prototype for monitoring membrane interaction due to its conformational plasticity. In this work, we comprehensively monitored the interaction of *apo*-BLA with zwitterionic and negatively charged membranes utilizing a variety of approaches. We show that BLA preferentially binds to negatively charged membranes at acidic pH with higher binding affinity. This is supported by spectral changes observed with a potential-sensitive membrane probe and fluorescence anisotropy measurements of a hydrophobic probe. Our results show that BLA exhibits a molten globule conformation when bound to negatively charged membranes. We further show, using the parallax approach, that BLA penetrates the interior of negatively charged membranes, and tryptophan residues are localized at the membrane interface. Red edge excitation shift (REES) measurements reveal that the immediate environment of tryptophans in membrane-bound BLA is restricted, and the restriction is dependent on membrane lipid composition. We envision that understanding the mechanism of BLA–membrane interaction would help in bioengineering of α-lactalbumin, and to address the mechanism of tumoricidal and antimicrobial activities of BLA–oleic acid complex.

© 2014 Elsevier B.V. All rights reserved.

1. Introduction

Bovine α-lactalbumin (BLA) is a small acidic Ca^{2+}-binding protein (mol. wt. 14.2 kDa) present in milk and it functions as a specificity modifier of galactosyltransferase [1]. Interestingly, BLA serves as a useful model for the protein folding problem since it has several partially unfolded intermediate states and is known to be present in molten globule form under various conditions [2]. The molten globule state is an important intermediate in protein folding, and was initially proposed as a partly folded state with stable native-like secondary structure but lacking a specific tertiary structure [2,3]. BLA is extensively used to study the molten globule state since it assumes the molten globule conformation under various conditions such as acidic pH and in the *apo*-state [1–5]. The *apo*-state molten globule is generated by removal of Ca^{2+} at neutral pH and low ionic strength in a narrow range of temperature [2]. BLA is intrinsically fluorescent due to the presence of four tryptophans (at positions 26, 60, 104 and 118) out of which Trp-118 belongs to aromatic cluster I, while the other three tryptophan residues are part of aromatic cluster II [6]. These suitably positioned tryptophans in BLA act as convenient probes to explore conformation and dynamics under various conditions [4,5]. Importantly, tryptophan residues have been reported to be crucial for the global stability of α-lactalbumin [7].

An interesting feature of BLA is that it interacts with membranes although it is a soluble protein [8]. Many soluble proteins are known to interact with membranes in partially disordered states, and the mechanism and relevance of such interactions in cellular processes are beginning to be understood. The transition of the protein from soluble to the membrane-associated state is believed to be associated with physiologically relevant conformational changes [9]. BLA interacts with membranes and this interaction is governed by the charge of the lipid headgroup, membrane curvature, composition, ionic strength and pH [8]. Earlier reports on BLA–membrane interaction mainly focused on membranes containing zwitterionic phosphatidylcholine (PC) [10–13]. It was later shown that BLA interacts with membranes containing negatively charged lipids such as phosphatidylglycerol (PG), although such interaction has not been characterized in detail [14–19].

The interaction of BLA with membranes assumes relevance since it has been reported that the complex of α-lactalbumin with oleic acid

Abbreviations: 2-AS, 2-(9-anthroyloxy)stearic acid; 12-AS, 12-(9-anthroyloxy)stearic acid; 5-PC, 1-palmitoyl-2-(5-doxyl)stearoyl-*sn*-glycero-3-phosphocholine; 12-PC, 1-palmitoyl-2-(12-doxyl)stearoyl-*sn*-glycero-3-phosphocholine; BLA, bovine α-lactalbumin; CD, circular dichroism; Di-8-ANEPPS, 4-(2-(6-(dioctylamino)-2-naphthalenyl)ethenyl)-1-(3-sulfopropyl)-pyridinium inner salt; DMPC, 1,2-dimyristoyl-*sn*-glycero-3-phosphocholine; DOPC, 1,2-dioleoyl-*sn*-glycero-3-phosphocholine; DOPG, 1,2-dioleoyl-*sn*-glycero-3-phosphatidylglycerol; DPH, 1,6-diphenyl-1,3,5-hexatriene; LUV, large unilamellar vesicle; PC, phosphatidylcholine; PG, phosphatidylglycerol; POPC, 1-palmitoyl-2-oleoyl-*sn*-glycero-3-phosphocholine; POPG, 1-palmitoyl-2-oleoyl-*sn*-glycero-3-phosphatidylglycerol; REES, red edge excitation shift; Tempo-PC, 1,2-dioleoyl-*sn*-glycero-3-phosphotempocholine

* Corresponding author. Tel.: +91 40 2719 2578; fax: +91 40 2716 0311.
E-mail address: amit@ccmb.res.in (A. Chattopadhyay).

http://dx.doi.org/10.1016/j.bbamem.2014.04.027
0005-2736/© 2014 Elsevier B.V. All rights reserved.

has tumoricidal and antimicrobial properties [20–25]. The ability of such complexes to differentiate between healthy and tumor cells remains an intriguing issue. On an average, ~30% of the total phospholipids in eukaryotic cell membranes contain negatively charged headgroups [26]. Anionic phospholipids play a major role in lipid–protein interactions, and in membrane insertion and translocation of proteins [26–29]. In this work, we comprehensively monitored the interaction of *apo*-BLA with zwitterionic membranes containing PC, and negatively charged membranes containing a mixture of PC/PG phospholipids. Our results, utilizing fluorescence from BLA tryptophans and from a potential-sensitive membrane probe, show that *apo*-BLA preferentially binds to negatively charged membranes with higher affinity in acidic pH. As a measure of the interaction of BLA with negatively charged membranes, we determined the depth of penetration of BLA tryptophans in the membrane interior using the parallax analysis. Interestingly, BLA tryptophans display differential extents of red edge excitation shift (REES) in zwitterionic and negatively charged membranes, clearly showing the difference in microenvironment in terms of restriction to solvent mobility.

2. Materials and methods

2.1. Materials

POPC, DOPG, DOPC, POPG, Tempo-PC, 5-PC, and 12-PC were obtained from Avanti Polar Lipids (Alabaster, AL). Calcium depleted BLA (*apo*-BLA), DPH and DMPC were from Sigma Chemical Co. (St. Louis, MO). 2-AS, 12-AS and di-8-ANEPPS were purchased from Molecular Probes/Invitrogen (Eugene, OR). Lipids were checked for purity by thin layer chromatography on silica gel precoated plates obtained from Merck (Darmstadt, Germany) in chloroform/methanol/water (65:35:5, v/v/v) and were found to give a single spot in all cases when visualized upon charring with a solution containing cupric sulfate (10%, w/v) and phosphoric acid (8%, v/v) at 150 °C [30]. The concentrations of phospholipids were determined by phosphate assay subsequent to total digestion by perchloric acid [31]. DMPC was used as an internal standard to assess lipid digestion. All other chemicals used were of the highest purity available. Solvents used were of spectroscopic grade. Water was purified through a Millipore (Bedford, MA) Milli-Q system and used throughout. Concentrations of stock solutions of di-8-ANEPPS and DPH in methanol were estimated from their molar extinction coefficients (ε) of 37,000 M^{-1} cm^{-1} at 498 nm [32], and 88,000 M^{-1} cm^{-1} at 350 nm [33], respectively. The concentration of BLA in water was estimated using the molar extinction coefficient (ε) of 28,540 M^{-1} cm^{-1} at 280 nm [34].

2.2. Methods

2.2.1. Sample preparation

All experiments (except depth measurements) were performed using large unilamellar vesicles (LUVs) of 100 nm diameter of POPC or 70% POPC/30% POPG (mol/mol). BLA concentration was kept constant at 2 μM, while the lipid concentration ranged from 20 to 400 μM for binding experiments utilizing tryptophan fluorescence. In experiments utilizing di-8-ANEPPS and DPH, the total lipid and probe concentrations were 200 and 4 μM, respectively (i.e., the probe concentration was 2 mol% in both cases). For LUV preparation, lipids (POPC or POPC/POPG) were mixed well and dried under a stream of nitrogen while being warmed gently (~35 °C). After further drying under a high vacuum for at least 3 h, the lipid mixture was hydrated (swelled) by addition of 1 ml of 10 mM citrate buffer (pH 5), and each sample was vortexed for 3 min to uniformly disperse the lipids to form homogeneous multilamellar vesicles. LUVs of 100 nm diameter were prepared by the extrusion technique using an Avestin Liposofast Extruder (Ottawa, Ontario, Canada) as previously described [35]. Briefly, the multilamellar vesicles were freeze-thawed five times using liquid nitrogen to ensure solute equilibration between trapped and bulk solutions and then extruded through polycarbonate filters (pore diameter of 100 nm) mounted in an extruder fitted with Hamilton syringes (Hamilton Company, Reno, NV). Samples were subjected to 11 passes through the polycarbonate filters to give the final LUV suspension. Background samples for experiments were prepared the same way except that no probe was added to them. Samples were incubated in dark for 12 h at room temperature (~23 °C) for equilibration before measuring fluorescence. All experiments were done with multiple sets of samples at room temperature (~23 °C).

2.2.2. Binding studies utilizing tryptophan fluorescence

Steady state fluorescence measurements were performed with a Hitachi F-7000 spectrofluorometer (Tokyo, Japan) using 1 cm path length quartz cuvette. Excitation and emission slits with a nominal bandpass of 2.5 nm were used for all measurements. Background intensities of samples in which protein was omitted were subtracted from each sample spectrum to cancel out any contribution due to the solvent Raman peak and other scattering artifacts. The spectral shifts obtained with different sets of samples were identical in most cases, or were within ±1 nm of the ones reported. The integrated area (F) under the tryptophan fluorescence spectra of BLA in solution was subtracted from the integrated spectral area of tryptophan fluorescence of BLA in the presence of lipid vesicles to calculate the difference (ΔF) at each lipid concentration. This difference (ΔF) was normalized to the integrated area (F) under the tryptophan fluorescence spectra of BLA in solution for each lipid concentration, and ΔF/F was calculated in each case. The data obtained was fitted to a simple hyperbolic function, which describes a single binding site model according to the following equation utilizing Sigma Plot (Systat Software Inc., San Jose, CA):

$$\Delta F/F = B_{max}[\text{Lipid}]/(K_d + [\text{Lipid}]) \quad (1)$$

where B_{max} is the maximum binding and K_d is the apparent dissociation constant.

2.2.3. Binding studies utilizing di-8-ANEPPS fluorescence

Fluorescence excitation spectra were recorded using a Hitachi F-7000 spectrofluorometer (Tokyo, Japan) with 1 cm path length quartz cuvette. Emission wavelength was fixed at 670 nm. Excitation and emission slits with a nominal bandpass of 2.5 nm were used for all measurements. Background intensities of samples were subtracted from each sample to cancel any contribution due to the solvent Raman peak and other scattering artifacts. The fluorescence ratio (R), defined as the ratio of fluorescence intensities at an excitation wavelength of 455 nm to that at 525 nm (emission at 670 nm in both cases) which is a measure of membrane dipole potential, was calculated from di-8-ANEPPS excitation spectra [36–38]. The choice of the emission wavelength (670 nm) at the red edge of the spectrum has previously been shown to rule out the membrane fluidity effects [37]. Normalized fluorescence ratio $R_{455/525}$ was obtained by dividing the fluorescence ratio (R) obtained in the presence of various concentrations of BLA in the presence of lipid vesicles with the fluorescence ratio obtained with only the probe (di-8-ANEPPS) in the membrane. The normalized $R_{455/525}$ for each concentration of BLA was plotted and fitted to a simple hyperbolic function utilizing Sigma Plot (Systat Software Inc., San Jose, CA) using the following equation:

$$\text{Normalized } R_{455/525} = 1 + (B_{max}[\text{BLA}])/(K_d + [\text{BLA}]) \quad (2)$$

which describes a single binding site model where K_d is the apparent dissociation constant and B_{max} corresponds to the maximum value of $R_{455/525}$.

2.2.4. Fluorescence anisotropy and REES measurements

DPH fluorescence anisotropy measurements were performed at room temperature (~23 °C) using a Hitachi polarization accessory in Hitachi F-7000 spectrofluorometer using 1 cm path length quartz

cuvettes. Fluorescence anisotropy values were calculated from the equation [39]:

$$r = \frac{I_{VV} - GI_{VH}}{I_{VV} + 2GI_{VH}} \quad (3)$$

where I_{VV} and I_{VH} are the measured fluorescence intensities (after appropriate background subtraction) with the excitation polarizer vertically oriented and emission polarizer vertically and horizontally oriented, respectively. G is the grating correction factor and is the ratio of the efficiencies of the detection system for vertically and horizontally polarized light, and is equal to I_{HV}/I_{HH}. The excitation wavelength was set at 358 nm, and emission was monitored at 430 nm. Excitation and emission slits with bandpasses of 2.5 nm were used for all measurements. The optical density of the samples measured at 358 nm was less than 0.2. All experiments were performed with at least three sets of samples and average values are shown. The fluorescence anisotropy for each concentration of BLA was plotted and fitted to a hyperbolic function (see above, Eq. (2)) utilizing Sigma Plot using the following equation:

$$\text{Fluorescence anisotropy} = 1 + (B_{max}[BLA])/(K_d + [BLA]). \quad (4)$$

REES measurements utilizing tryptophan fluorescence were performed in a Fluorolog-3 Model FL3-22 spectrofluorometer (Horiba Jobin Yvon, Edison, NJ). Excitation and emission slits with bandpasses of 3 nm were used.

2.2.5. Depth measurements using the parallax method

The actual spin (nitroxide) contents of the spin-labeled phospholipids (Tempo-, 5- and 12-PC) were assayed using fluorescence quenching of anthroyloxy-labeled fatty acids (2- and 12-AS) as described previously [40]. Liposomes were made by the ethanol injection method [41,42] for depth measurements. These samples were made by co-drying 750 nmol of lipid (70% DOPC/30% DOPG, mol/mol) containing 10 mol% spin-labeled phospholipid (Tempo-, 5- or 12-PC) under a steady stream of nitrogen with gentle warming (~35 °C), followed by further drying under a high vacuum for at least 3 h. The dried lipid film was dissolved in ethanol to give a final concentration of 40 mM. The ethanolic lipid solution was then injected into 1 mL of 10 mM citrate buffer (pH 5), while vortexing to give a final concentration of 750 μM lipid in buffer. *Apo*-BLA was incorporated into membranes by adding a small aliquot from a stock solution in water to the pre-formed vesicles such that the lipid to protein ratio was 300 (mol/mol). Duplicate samples were prepared in each case except for samples lacking the quencher for which triplicates were prepared. Background samples lacking BLA were prepared in all experiments, and their fluorescence intensity was subtracted from the respective sample fluorescence intensity in each case. Samples were kept in the dark for 12 h before measuring fluorescence.

2.2.6. Circular dichroism (CD) measurements

CD measurements were carried out at room temperature (~23 °C) on a JASCO J-815 spectropolarimeter (Tokyo, Japan) which was calibrated with (+)-10-camphorsulfonic acid [43]. Spectra were scanned in a quartz optical cell with a path length of 0.1 cm for far-UV and 1 cm for near-UV range, and recorded in 0.5 nm wavelength increments and band width of 2 nm. For monitoring changes in secondary and tertiary structures, spectra were scanned from 200 to 250 nm in the far-UV range, and from 250 to 300 nm in the near-UV range, respectively. The scan rate was 50 nm/min and each spectrum was the average of 4 scans with a full scale sensitivity of 100 mdeg. Spectra were corrected for background by subtraction of appropriate blanks. Data are represented as mean residue ellipticities and calculated using the equation:

$$[\theta] = \theta_{obs}/(10Cl) \quad (5)$$

where θ_{obs} is the observed ellipticity in mdeg, l is the path length in cm, and C is the concentration of peptide bonds in mol/L.

3. Results

3.1. BLA binds to negatively charged membranes with higher affinity

We utilized BLA tryptophan fluorescence to monitor its binding to membranes of varying charge. Fig. 1 shows the fluorescence emission spectra of BLA in negatively charged (panel a) and zwitterionic (panel b) membranes with increasing lipid/protein (mol/mol) ratio. Fig. 1a shows that there is a considerable increase in fluorescence intensity of BLA with increasing lipid/protein ratio in case of negatively charged membranes. The increase in fluorescence upon binding could be due to conformational changes resulting in the release of quenching of some of the tryptophan residues of BLA. BLA has four tryptophans [6] and an increase in fluorescence intensity has previously been reported upon partial unfolding into the molten globule state from the native (ordered) conformation [4,5]. Interestingly, such an increase in BLA fluorescence intensity is not observed in case of zwitterionic membranes with increasing lipid/protein ratio (see Fig. 1b). This is due to much weaker binding of BLA to zwitterionic membranes. The inset in Fig. 1b shows emission spectra in all cases (soluble and in the presence of membranes).

In order to analyze these results more quantitatively and determine binding affinity, we analyzed the binding plot of *apo*-BLA with

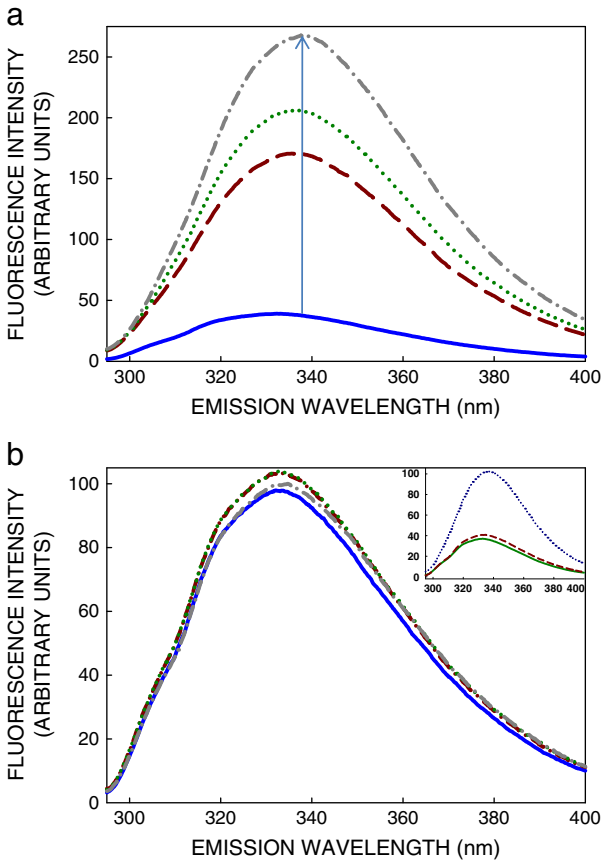

Fig. 1. Representative fluorescence emission spectra of *apo*-BLA in (a) negatively charged (POPC/POPG), and (b) zwitterionic (POPC) membranes, corresponding to lipid to protein ratio (mol/mol) of 10 (——); 25 (- - -); 50 (· · · ·) and 150 (- · -). The concentration of *apo*-BLA was 2 μM in all cases. The arrow in panel (a) indicates significant increase in BLA fluorescence intensity upon binding to negatively charged membranes. The inset in (b) shows the emission spectra of *apo*-BLA in buffer (——), negatively charged (- - -) and zwitterionic (· · · ·) membranes (the lipid/protein ratio was 150 (mol/mol) in case of membrane samples). See Materials and methods for other details.

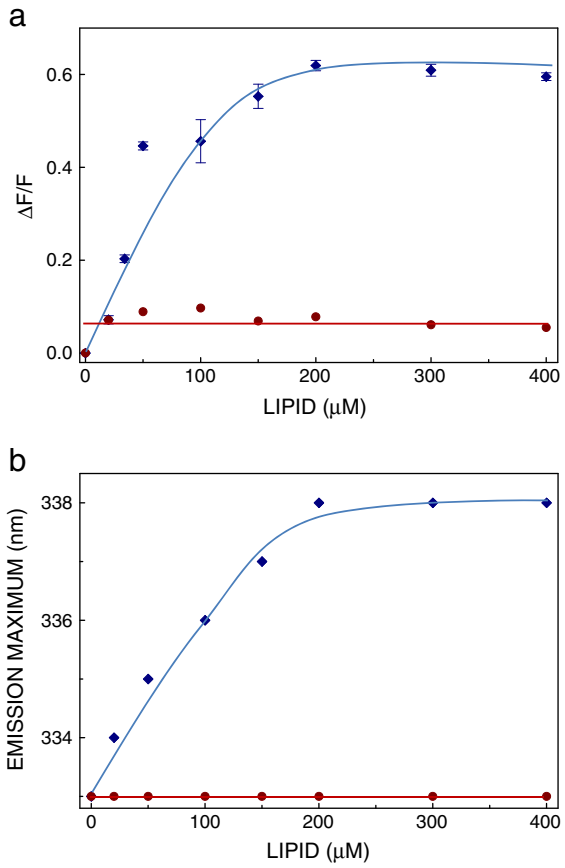

Fig. 2. (a) Binding plot of *apo*-BLA with membranes utilizing tryptophan fluorescence. Normalized difference in the spectral areas (ΔF/F) of tryptophan emission spectrum of *apo*-BLA in the presence of negatively charged (♦) and zwitterionic (●) membranes with increasing concentration of total lipid are shown. The concentration of *apo*-BLA was 2 μM. Normalized differences in the spectral areas (ΔF/F) shown are means ± S.E. of at least three independent measurements. The apparent dissociation constant for binding of *apo*-BLA to negatively charged membranes obtained upon fitting the data points is shown in Table 1. Lines joining the data points are provided merely as viewing guides. (b) Change in tryptophan fluorescence emission maximum of *apo*-BLA upon interaction with negatively charged (♦) and zwitterionic (●) membranes. The excitation wavelength used was 280 nm. Lines joining the data points are provided merely as viewing guides. See Materials and methods for other details.

membranes of varying charges utilizing tryptophan fluorescence. Fig. 2a shows the change in ΔF/F (see Materials and methods for details) with increasing lipid concentration. Data for BLA binding to negatively charged membranes was fitted to a single binding site hyperbola which yielded an apparent dissociation constant (K_d) of ~27 μM (see Table 1). The corresponding plot of ΔF/F vs. lipid concentration for zwitterionic membranes implies no significant binding and did not yield any dissociation constant. Fig. 2b shows the corresponding change in fluorescence emission maximum with lipid concentration. In case of negatively charged membranes, the emission maximum[1] of *apo*-BLA exhibits a red shift of 5 nm (from 333 to 338 nm) with increasing lipid/protein ratio due to binding. In contrast, the emission maximum remains invariant at 333 nm upon increasing lipid/protein ratio in case of zwitterionic membranes, in agreement with Fig. 2a. This red shift could be due to partial unfolding to the molten globule state upon membrane binding.

[1] We have used the term maximum of fluorescence emission in a somewhat broader sense here. In every case, we have monitored the wavelength corresponding to maximum fluorescence intensity, as well as the center of mass of the fluorescence emission, in the symmetric part of the spectrum. In most cases, both these methods yielded the same wavelength. In cases where minor discrepancies were found, the center of mass of emission has been reported as the fluorescence maximum.

Table 1
Binding of *apo*-BLA to negatively charged membranes.

Apparent Dissociation Constant (K_d)[a] (from tryptophan fluorescence) (μM)	27.1 ± 1.8
Apparent Dissociation Constant (K_d)[b] (from di-8-ANEPPS fluorescence) (μM)	3.7 ± 0.1
Apparent Dissociation Constant (K_d)[c] (from DPH anisotropy) (μM)	11.0 ± 2.0

Data shown are means ± S.E. of at least three independent measurements. See Materials and methods for other details.
[a] Calculated using Eq. (1).
[b] Calculated using Eq. (2).
[c] Calculated using Eq. (4).

Dipole potential has previously been reported to be a sensitive tool to monitor interaction of peptides and proteins with membranes [36,44–46]. Dipole potential is the potential difference within the membrane bilayer, which originates due to the nonrandom arrangement of lipid dipoles and water molecules at the membrane interface. In order to complement our binding experiments utilizing tryptophan fluorescence, we monitored BLA binding to membranes using di-8-ANEPPS, a potential-sensitive membrane probe which localizes at the membrane interface [38]. The excitation spectrum of di-8-ANEPPS is sensitive to alterations in membrane dipole potential. Representative normalized fluorescence excitation spectra of di-8-ANEPPS in negatively charged membranes in the presence and absence of BLA are shown in Fig. S1. Fluorescence difference spectra were plotted to determine the changes resulting from spectral shifts in the excitation spectra, by subtracting the normalized spectrum of the probe bound to membranes (PC/PG) containing BLA from the spectrum of only the probe bound to membranes [44,47]. Fig. 3a shows the difference spectra of di-8-ANEPPS, in the presence of BLA bound to negatively charged membranes, display distinct spectral features, i.e., a peak at ~515 nm and a trough at ~430 nm in the presence of 4 μM (corresponding to lipid to protein ratio of 50) and higher BLA concentrations. Such positions of the peak and trough in the difference spectra indicate a decrease in the membrane potential [44,47] with BLA binding. We utilized the dual ratiometric approach [48], i.e. monitoring the ratio of the fluorescence intensity at 455 and 525 nm from the excitation spectra while fixing the emission wavelength at 670 nm, to probe membrane binding of BLA. Fig. 3b shows that this normalized fluorescence ratio displays considerable reduction (~60%) in negatively charged membranes, at the highest BLA concentration (20 μM). The change in the fluorescence ratio is much less (~10%) in case of zwitterionic membranes at the highest BLA concentration used. The reduction in normalized $R_{455/525}$ of di-8-ANEPPS in negatively charged membranes with increasing concentration of BLA followed a hyperbolic curve. This data was analyzed according to single binding site model to yield an apparent dissociation constant (K_d) of ~3.7 μM (see Table 1). These results suggest that the binding of BLA to negatively charged membranes causes membrane perturbation, as sensed by the potential-sensitive probe di-8-ANEEPS.

We also monitored the interaction of BLA with membranes utilizing DPH fluorescence anisotropy. DPH is a rigid hydrophobic rod-shaped molecule and partitions into the interior of the bilayer. It is a popular membrane probe for monitoring membrane organization and dynamics [49], and for monitoring packing changes induced in membranes as a result of protein or peptide binding [50]. The change in DPH anisotropy with increasing BLA concentration (i.e., decreasing lipid/protein ratio) is shown in Fig. 4. As shown in the figure, DPH anisotropy remains invariant in case of zwitterionic membranes. In contrast, DPH anisotropy displays a concentration-dependent increase in negatively charged membranes, beyond BLA concentration of 1 μM (corresponding to lipid/protein ratio of 200 (mol/mol)). We attribute the increase in DPH anisotropy (due to increased membrane ordering) to specific binding of BLA to negatively charged membranes under these conditions (see Fig. 2). The apparent dissociation constant of BLA binding to negatively charged membranes

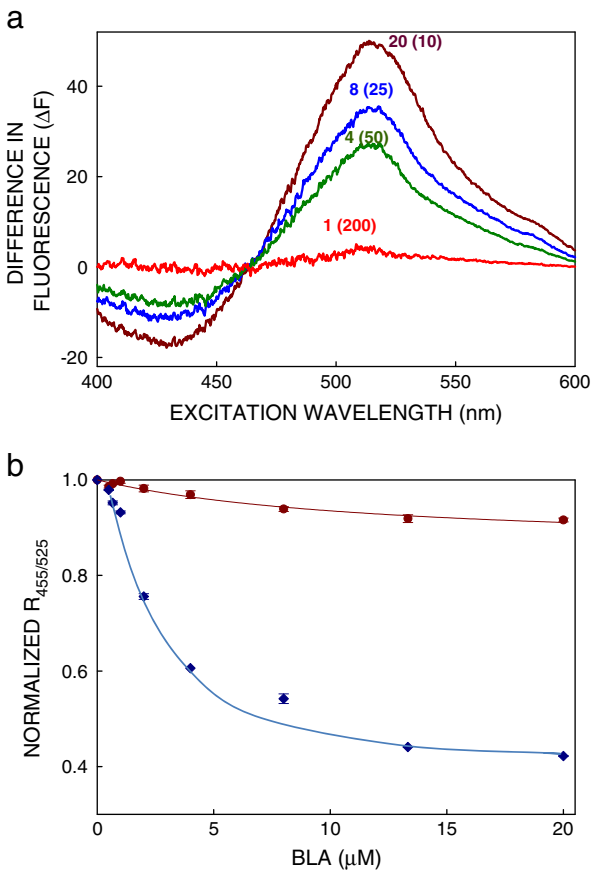

Fig. 3. Membrane interaction of *apo*-BLA monitored using the fluorescence of the potential-sensitive probe di-8-ANEPPS. (a) Fluorescence difference spectra obtained by subtracting di-8-ANEPPS excitation spectra in negatively charged membranes from di-8-ANEPPS excitation spectra obtained after addition of 1, 4, 8, and 20 μM of *apo*-BLA. These correspond to lipid/protein (mol/mol) ratio of 200, 50, 25 and 10, respectively. Each difference spectrum is labeled with the concentration of *apo*-BLA and the corresponding lipid/protein (mol/mol) ratio in the figure. (b) Binding plot of *apo*-BLA with negatively charged and zwitterionic membranes utilizing the fluorescence of the potential-sensitive probe di-8-ANEPPS. Normalized change in fluorescence ratio ($R_{455/525}$) of the excitation spectra of di-8-ANEPPS in negatively charged (♦) and zwitterionic (●) membranes with increasing *apo*-BLA concentration are shown. The normalized fluorescence ratios shown are means ± S.E. of at least three independent measurements. The concentration of phospholipids and di-8-ANEPPS were 200 and 4 μM, respectively. The apparent dissociation constant for binding of *apo*-BLA to negatively charged membranes obtained upon fitting the data points is shown in Table 1. Lines joining the data points are provided merely as viewing guides. See Materials and methods for other details.

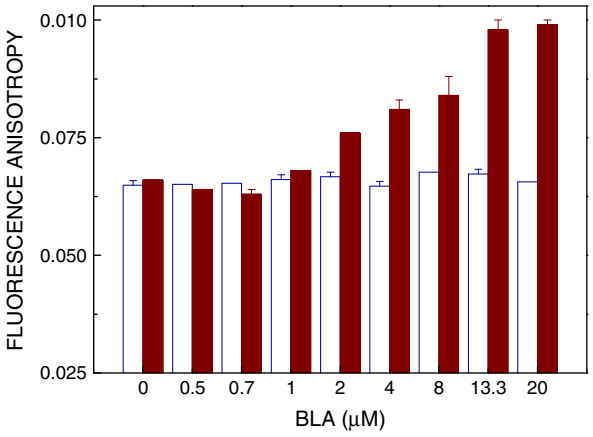

Fig. 4. Effect of increasing *apo*-BLA concentration on fluorescence anisotropy of membrane embedded DPH in negatively charged (solid bar) and zwitterionic (empty bar) membranes. Fluorescence anisotropy data shown are means ± S.E. of at least three independent measurements. Excitation and emission wavelengths were set at 358 and 430 nm. Concentrations of lipid and DPH were 200 and 4 μM, respectively. See Materials and methods for other details.

from DPH anisotropy data analyzed according to the single binding site model was found to be ~11 μM (see Table 1 and Fig. S2).

Table 1 shows that the apparent dissociation constants of *apo*-BLA binding to negatively charged membranes are somewhat different, depending on the approach and probe used. This observation merits comment. The table shows that while the dissociation constant obtained using tryptophan fluorescence is relatively high (27.1 μM), the corresponding value utilizing di-8-ANEPPS is low (3.7 μM). The value of dissociation constant using DPH anisotropy data (11 μM) interestingly is between these two values. The dissociation constant obtained utilizing environment-sensitive tryptophan fluorescence reflects binding in terms of local changes in the microenvironment of the tryptophans induced by membrane binding. On the other hand, the apparent dissociation constant obtained utilizing the potential-sensitive di-8-ANEPPS fluorescence reflects change in the dipole potential of the membrane (due to reorientation of membrane dipoles) brought about by binding of BLA to the membrane. The dissociation constant obtained utilizing DPH anisotropy is indicative of changes in lipid packing (reported by DPH anisotropy) due to BLA binding. It should be noted that the value derived from tryptophan fluorescence will be influenced by the relative accessibility of the individual tryptophans in a multi-tryptophan protein such as BLA, and the complexity associated with differential quantum yield among tryptophans due to environmental sensitivity of fluorescence. On the other hand, the bilayer location of di-8-ANEPPS and DPH is different and this difference could manifest in dissociation constants.

3.2. Conformational change of BLA upon membrane binding

We utilized near- and far-UV CD spectroscopy to monitor secondary and tertiary conformations of BLA upon binding to membranes. Fig. 5a shows that the spectral characteristics of the secondary structure of *apo*-BLA, upon binding to negatively charged membranes, exhibit an enhancement of far-UV CD bands (~208 and 222 nm), indicating increased helicity under these conditions. Fig. 5b shows a considerable loss of tertiary structure of *apo*-BLA upon binding to negatively charged membranes, relative to zwitterionic membranes. The loss of tertiary structure, along with the presence of secondary structure, is a hallmark of molten globule conformation, adopted by BLA upon binding to negatively charged membranes. These features are absent in far- and near-UV CD spectra of BLA in zwitterionic membranes. These results imply that BLA adopts molten globule conformation only in the presence of negatively charged membranes. The far- and near-UV CD spectra of *apo*-BLA in buffer are also shown for comparison.

3.3. Restricted microenvironment of BLA tryptophans in membranes monitored by REES

REES is operationally defined as the shift in the wavelength of maximum fluorescence emission toward higher wavelengths, caused by a shift in the excitation wavelength toward the red edge of the absorption band. REES assumes relevance for polar fluorophores in motionally restricted environment where the dipolar relaxation time for the solvent shell around a fluorophore becomes comparable to or longer than its fluorescence lifetime [51–56]. A unique aspect of REES is that it allows to monitor the mobility parameters of the environment itself (represented by the relaxing solvent molecules) using the fluorophore merely as a reporter group. REES has proved to be a convenient tool to monitor organization and dynamics of probes and proteins in membranes and membrane-mimetic environments [57–63].

Fig. 6 shows the shifts in the maxima of fluorescence emission of *apo*-BLA in membranes as a function of excitation wavelength. The

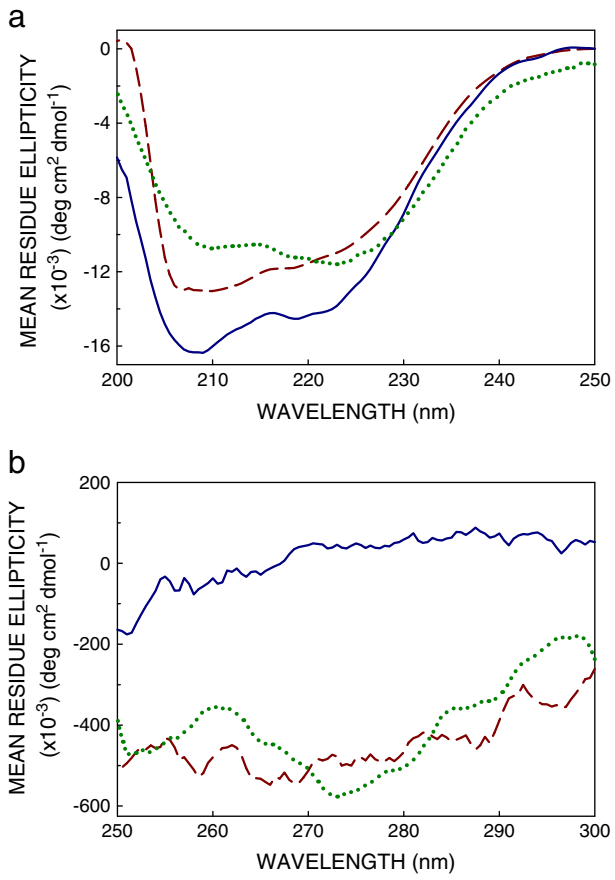

Fig. 5. Representative (a) far-UV and (b) near-UV CD spectra of *apo*-BLA in negatively charged (—) and zwitterionic (- - -) membranes. The concentration of *apo*-BLA was 10 μM for both cases, and the lipid to protein ratio was 200 (mol/mol). The far- and near-UV CD spectra of *apo*-BLA in buffer (····) are also shown. The concentration of *apo*-BLA used was 2 and 10 μM for far- and near-UV CD, respectively. See Materials and methods for other details.

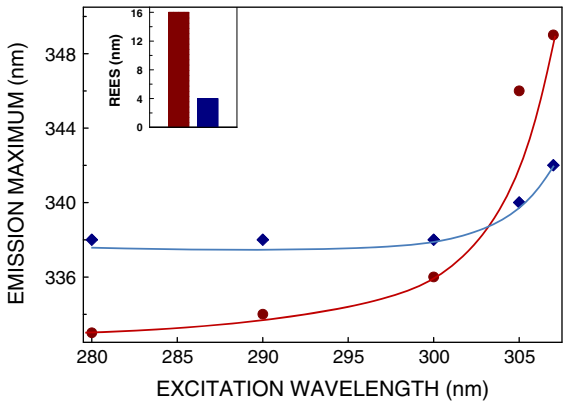

Fig. 6. Effect of changing excitation wavelength on the wavelength of maximum emission of tryptophan residues of *apo*-BLA in negatively charged (♦) and zwitterionic (●) membranes. Lines joining the data points are provided merely as viewing guides. The inset shows the magnitude of REES in both cases, which corresponds to the total shift in emission maximum when the excitation wavelength was changed from 280 to 307 nm (the left bar corresponds to zwitterionic membranes). The lipid to protein ratio was 200 (mol/mol) and *apo*-BLA concentration was 2 μM in both cases. See Materials and methods for other details.

figure shows that the emission maximum of BLA in zwitterionic membranes is shifted from 333 to 349 nm in response to a change in excitation wavelength from 280 to 307 nm, corresponding to REES of 16 nm (shown in inset). In contrast to this, BLA in negatively charged membranes displays a relatively modest shift from 338 to 342 nm, which corresponds to REES of 4 nm (see inset). Such characteristic dependence of the emission maximum on excitation wavelength is typical of REES. It is possible that there could be further red shift upon excitation at longer wavelengths beyond 307 nm. However, we found it difficult to work in this wavelength range because of very low signal to noise ratio and artifacts due to the solvent Raman peak that sometimes persisted even after background subtraction. The relatively small REES observed for BLA in negatively charged membranes could be due to faster solvent relaxation around the tryptophan residues in the molten globule conformation, adopted by BLA in negatively charged membranes (see Fig. 5). We have previously reported that the molten globule conformation of BLA exhibits reduced REES relative to the corresponding value in native conformation [5]. In contrast, REES exhibited by BLA in zwitterionic membranes is relatively high probably due to the compactness of BLA (see Fig. 5) with no loss of folding. We carried out REES measurements with few points since including more data points in the plot does not always help, keeping in mind the error in emission wavelength created due to finite band width. In addition, significant REES is only observed when excitation is carried out >300 nm, a range of excitation wavelength where signal/noise ratio of the spectrum becomes increasingly poor.

3.4. Depth of penetration of BLA tryptophans upon binding to negatively charged membranes

Membrane penetration depth [64–66] is an important parameter in the study of membrane peptides [57] and proteins [67], since knowledge of the depth of a membrane embedded group helps define the conformation and topology of membrane-bound molecules.

To explore the extent of BLA–membrane interaction, we determined the penetration depth of BLA tryptophans in negatively charged membranes using the parallax approach [64]. The average depth of BLA tryptophans were calculated using the equation:

$$z_{cF} = L_{c1} + \left\{ \left[(-1/\Pi C) \ln(F_1/F_2) - L_{21}^2 \right] / 2\, L_{21} \right\} \quad (6)$$

where z_{cF} is the distance of the fluorophore from the center of the bilayer, L_{c1} is the distance of the center of the bilayer from the shallow quencher, L_{21} is the difference in depth between the two quenchers (i.e., the vertical distance between the shallow and deep quenchers), and C is the two dimensional quencher concentration (molecules/Å^2) in the plane of the membrane. Here, F_1/F_2 is the ratio of F_1/F_o and F_2/F_o, in which F_1 and F_2 are the fluorescence intensities in the presence of the shallow quencher and the deep quencher, respectively, both at the same quencher concentration C; F_o is the fluorescence intensity in the absence of any quencher. All the bilayer parameters used were the same as described previously [64]. Analysis of quenching data show that the average depth of penetration of BLA tryptophans is ~13 Å from the center of the bilayer (see Table 2). These results suggest that the tryptophan residues in negatively charged membrane-bound BLA are localized at the interfacial region of the membrane. This is in agreement with the membrane anchoring property of tryptophans in a number of peptides and proteins which requires an interfacial localization [55,69–73].

4. Discussion

The interaction of soluble proteins with membranes represents a fundamental process underlying many biological events such as the action of bacterial and viral toxins [9,74–76], binding of seminal plasma proteins to sperm plasma membranes [77], and etiology of neurodegenerative disorders such as Parkinson's disease [78]. However, the understanding of the molecular details of the interaction of soluble proteins with membranes is still an emerging area. Elucidation of the mechanism

Table 2
Average membrane penetration depths of tryptophans of *apo*-BLA in negatively charged membranes.[a]

Spin-labeled PC pair used for quenching analysis	Calculated distance from the bilayer center z_{cF} (Å)	Average z_{cF} (Å)[b]
Tempo-PC/5-PC	15.0	12.8
5-PC/12-PC	10.6	

[a] Depths were calculated from fluorescence quenchings obtained with samples containing 10 mol% of Tempo-, 5- or 12-PC and using Eq. (6). Samples were excited at 295 nm, and emission was collected at 335 nm. The ratio of *apo*-BLA to total lipid was 1:300 (mol/mol) and the concentration of BLA was 2.5 μM in all cases. See Materials and methods for other details.
[b] The strongest quenching was observed with 5-PC. Since the levels of Tempo-PC and 12-PC quenchings were indistinguishable within experimental error (<5% difference in relative fluorescence intensity, i.e., $0.95 < F_{12\text{-PC}}/F_{\text{Tempo-PC}} < 1.05$), it was necessary to average z_{cF} values in order to get accurate depth [40]. We further confirmed the calculation of depth by polynomial analysis [68] (data not shown).

of soluble protein–membrane interaction assumes relevance since it allows designing of therapeutically useful agents such as toxin-immunoglobulin hybrids (immunotoxins). A number of studies have shown that partial unfolding is a crucial common feature in the interaction and translocation of soluble proteins [9,79]. BLA represents an excellent prototype for monitoring membrane interaction due to its conformational plasticity.

In this work, we explored the interaction of *apo*-BLA with zwitterionic (PC) and negatively charged (PC/PG) membranes utilizing a variety of biophysical approaches. The major thrust of our work is on quantitative determination of BLA binding to zwitterionic and negatively charged membranes utilizing both lipid-bound and protein associated probes. Our results provide, for the first time, binding analysis of BLA to membranes utilizing lipid probes such as the potential-sensitive probe di-8-ANEPPS which is increasingly becoming a popular probe for measurement of membrane dipole potential [38]. In the process, we utilized sensitive fluorescence approaches such as REES to address the solvent restriction experienced by BLA tryptophans upon interaction with membranes. To the best of our knowledge, our results constitute the first report in which BLA–membrane interaction has been monitored using REES. Another novel aspect of our work is the measurement of the penetration depth of BLA when bound to negatively charged membranes using the parallax approach. Our results, utilizing intrinsic fluorescence of BLA, show that BLA preferentially binds to negatively charged membranes at acidic pH with a binding affinity corresponding to a dissociation constant in ~μM range. These conclusions are supported by spectral changes observed with a voltage-sensitive membrane probe di-8-ANEPPS, which monitors changes in membrane dipole potential upon binding, and changes in fluorescence anisotropy of the hydrophobic probe DPH. CD spectra of BLA in negatively charged membranes (but not in zwitterionic membranes) show that the protein adopts molten globule conformation. Analysis of membrane penetration depth using the parallax approach reveals that BLA tryptophan residues are localized at the membrane interface. The microenvironment of tryptophans in BLA appears to be restricted in terms of solvent relaxation (reorientation), since BLA tryptophans exhibit REES. Differential REES in zwitterionic and negatively charged membranes bring out the difference in microenvironment in terms of restriction to solvent mobility.

The average depths of the fluorescent groups in di-8-ANEPPS and DPH, the probes used in this study, from the membrane center are ~12 and 8 Å, respectively [38,68]. Fluorescence of both these probes displays changes in negatively charged membranes upon BLA binding. This indicates that interaction of BLA affects both the interfacial and the hydrophobic region of the membranes. This could be due to penetration of one or more of the BLA helices (helices A and C [16,80]) into the membrane. Such deep perturbation of the membrane was previously reported from motional restriction observed throughout the length of the lipid fatty acyl chain in the ESR spectra of spin-labeled PG [81].

Our results utilizing the parallax method provide an average interfacial localization of the tryptophan residues of BLA bound to negatively charged membranes. Careful inspection of earlier literature shows that out of the four tryptophans in BLA, only the backbone amide protons of Trp-104 displayed protection against solvent exchange in negatively charged membranes [16]. Interestingly, a previous study identified that the segment 80-108 of BLA, which contains Trp-104, was protected

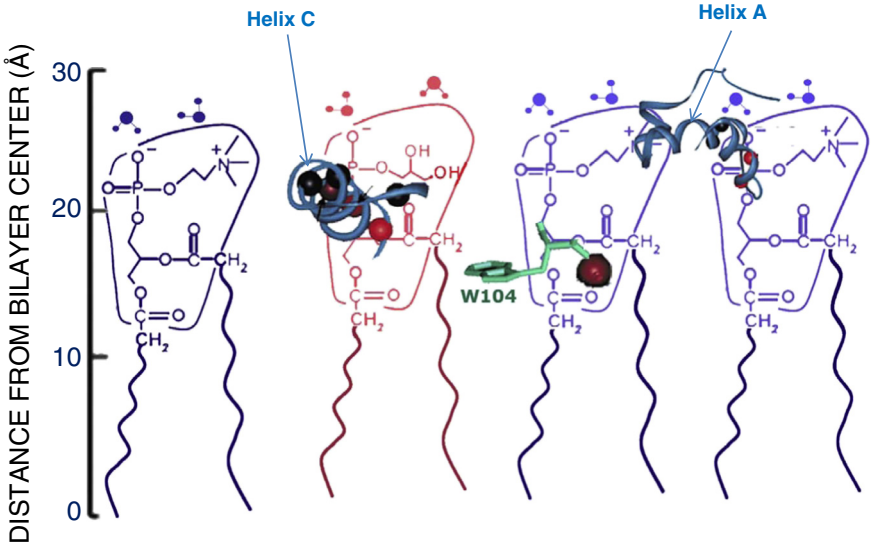

Fig. 7. A schematic representation of the membrane monolayer showing the orientation and location of segments of BLA (helix C, helix A and Trp-104): two types of lipids are shown in the membrane: zwitterionic (three in number, blue) and anionic (one in number, red). The residues represented by gradation of red color in segments of BLA are protected from backbone amide ^{1}H exchange, as monitored by NMR measurements upon binding to negatively charged membranes [16]. The brighter the shade of red, the greater is the protection of the amino acid residues upon binding to negatively charged membranes. The segments of BLA (helices A and C) are adapted and modified from Ref. [16]. The only tryptophan that is protected is Trp-104, and the location (depth) of this tryptophan is shown as measured by the parallax method (see Table 2). The shaded open triangles (△) represent interfacial (membrane-associated) water molecules. See text for other details.

from proteolytic cleavage upon binding to negatively charged membranes [80]. Based on these results, we speculate that Trp-104 is crucial for membrane interaction of BLA. Fig. 7 shows a putative model based upon penetration of helices A and C into negatively charged membranes. The residue Trp-104 is shown to be present at an interfacial depth of ~13 Å from the center of the membrane bilayer. It is interesting to note that Trp-104 in α-lactalbumins is conserved among various species since this residue is involved in the binding of α-lactalbumin to galactosyltransferase and the stimulation of its lactose synthase activity [82,83].

A recent study has shown that α-lactalbumin, when used as a vaccine, provides substantial protection and therapy against growth of tumors in transgenic mouse models of breast cancer [84]. Understanding the mechanism of interaction of α-lactalbumin with membranes would help in better bioengineering of α-lactalbumin, which could prove to be a promising anti-cancer agent for clinical usage. Current work in our laboratory is focused on finding other plasma membrane lipids that could be important for membrane interaction of BLA. A comprehensive knowledge of the interaction of BLA with specific lipids would be helpful to address the mechanism of tumoricidal and antimicrobial activities of BLA–oleic acid complex.

Acknowledgments

This work was supported by the Council of Scientific and Industrial Research, Govt. of India. Ar.C. thanks the Council of Scientific and Industrial Research for the award of a Senior Research Fellowship. A.C. is an Adjunct Professor at the Special Centre for Molecular Medicine of Jawaharlal Nehru University (New Delhi, India) and Indian Institute of Science Education and Research (Mohali, India), and Honorary Professor of the Jawaharlal Nehru Centre for Advanced Scientific Research (Bangalore, India). A.C. gratefully acknowledges support from J.C. Bose Fellowship (Department of Science and Technology, Govt. of India). We thank Hirak Chakraborty for useful discussions and help with analysis of binding data, and members of our laboratory for critically reading the manuscript.

Appendix A. Supplementary data

Supplementary data to this article can be found online at http://dx.doi.org/10.1016/j.bbamem.2014.04.027.

References

[1] E.A. Permyakov, L.J. Berliner, α-Lactalbumin: structure and function, FEBS Lett. 473 (2000) 269–274.
[2] K. Kuwajima, The molten globule state of α-lactalbumin, FASEB J. 10 (1996) 102–109.
[3] D.A. Dolgikh, R.I. Gilmanshin, E.V. Brazhnikov, V.E. Bychkova, G.V. Semisotnov, S.Y. Venyaminov, O.B. Ptitsyn, α-Lactalbumin: compact state with fluctuating tertiary structure? FEBS Lett. 136 (1981) 311–315.
[4] A. Chaudhuri, S. Haldar, A. Chattopadhyay, Organization and dynamics of tryptophans in the molten globule state of bovine α-lactalbumin utilizing wavelength-selective fluorescence approach: comparisons with native and denatured states, Biochem. Biophys. Res. Commun. 394 (2010) 1082–1086.
[5] D.A. Kelkar, A. Chaudhuri, S. Haldar, A. Chattopadhyay, Exploring tryptophan dynamics in acid-induced molten globule state of bovine α-lactalbumin: a wavelength-selective fluorescence approach, Eur. Biophys. J. 39 (2010) 1453–1463.
[6] E.D. Chrysina, K. Brew, K.R. Acharya, Crystal structures of apo- and holo-bovine α-lactalbumin at 2.2-Å resolution reveal an effect of calcium on inter-lobe interactions, J. Biol. Chem. 275 (2000) 37021–37029.
[7] A. Vanhooren, E. Illyes, Z. Majer, I. Hanssens, Fluorescence contributions of the individual Trp residues in goat α-lactalbumin, Biochim. Biophys. Acta 1764 (2006) 1586–1591.
[8] Ø. Halskau, A. Muga, A. Martínez, Linking new paradigms in protein chemistry to reversible membrane–protein interactions, Curr. Protein Pept. Sci. 10 (2009) 339–359.
[9] E. London, How bacterial toxins enter cells: the role of partial unfolding in membrane translocation, Mol. Microbiol. 6 (1992) 3277–3282.
[10] W. Herreman, P. van Tornout, F.H. van Cauwelaert, I. Hanssens, Interaction of α-lactalbumin with dimyristoyl phosphatidylcholine vesicles. II. A fluorescence polarization study, Biochim. Biophys. Acta 640 (1981) 419–429.
[11] I. Hanssens, J.-C. van Ceunebroeck, H. Pottel, G. Preaux, F. van Cauwelaert, Influence of the protein conformation on the interaction between α-lactalbumin and dimyristoylphosphatidylcholine vesicles, Biochim. Biophys. Acta 817 (1985) 154–164.
[12] A.K. Lala, P. Kaul, P.B. Ratnam, Membrane–protein interaction and the molten globule state: interaction of α-lactalbumin with membranes, Protein Chem. 14 (1995) 601–609.
[13] K.M. Cawthern, E. Permyakov, L.J. Berliner, Membrane-bound states of α-lactalbumin: implications for the protein stability and conformation, Protein Sci. 5 (1996) 1394–1405.
[14] S. Bañuelos, A. Muga, Binding of molten globule-like conformations to lipid bilayers. Structure of native and partially folded α-lactalbumin bound to model membranes, J. Biol. Chem. 270 (1995) 29910–29915.
[15] S. Bañuelos, A. Muga, Structural requirements for the association of native and partially folded conformations of α-lactalbumin with model membranes, Biochemistry 35 (1996) 3892–3898.
[16] Ø. Halskau, N.Å. Frøystein, A. Muga, A. Martínez, The membrane-bound conformation of α-lactalbumin studied by NMR-monitored ^{1}H exchange, J. Mol. Biol. 321 (2002) 99–110.
[17] A.V. Agasøster, Ø. Halskau, E. Fuglebakk, N.Å. Frøystein, A. Muga, H. Holmsen, A. Martínez, The interaction of peripheral proteins and membranes studied with α-lactalbumin and phospholipid bilayers of various compositions, J. Biol. Chem. 278 (2003) 21790–21797.
[18] I. Rødland, Ø. Halskau, A. Martínez, H. Holmsen, α-Lactalbumin binding and membrane integrity-effect of charge and degree of unsaturation of glycerophospholipids, Biochim. Biophys. Acta 1717 (2005) 11–20.
[19] A. Chenal, G. Vernier, P. Savarin, N.A. Bushmarina, A. Gèze, F. Guillain, D. Gillet, V. Forge, Conformational states and thermodynamics of α-lactalbumin bound to membranes: a case study of the effects of pH, calcium, lipid membrane curvature and charge, J. Mol. Biol. 349 (2005) 890–905.
[20] M. Svensson, A. Håkansson, A.-K. Mossberg, S. Linse, C. Svanborg, Conversion of α-lactalbumin to a protein inducing apoptosis, Proc. Natl. Acad. Sci. U. S. A. 97 (2000) 4221–4226.
[21] C. Svanborg, H. Agerstam, A. Aronson, R. Bjerkvig, C. Düringer, W. Fischer, L. Gustafsson, O. Hallgren, I. Leijonhuvud, S. Linse, A.-K. Mossberg, H. Nilsson, J. Pettersson, M. Svensson, HAMLET kills tumor cells by an apoptosis-like mechanism-cellular, molecular, and therapeutic aspects, Adv. Cancer Res. 88 (2003) 1–29.
[22] M. Svensson, J. Fast, A.-K. Mossberg, C. Düringer, L. Gustafsson, O. Hallgren, C.L. Brooks, L. Berliner, S. Linse, C. Svanborg, α-lactalbumin unfolding is not sufficient to cause apoptosis, but is required for the conversion to HAMLET (human α-lactalbumin made lethal to tumor cells), Protein Sci. 12 (2003) 2794–2804.
[23] J. Pettersson-Kastberg, S. Aits, L. Gustafsson, A. Mossberg, P. Storm, M. Trulsson, F. Persson, K.H. Mok, C. Svanborg, Can misfolded proteins be beneficial? The HAMLET case, Ann. Med. 41 (2009) 162–176.
[24] A.P. Hakansson, H. Roche-Hakansson, A.-K. Mossberg, C. Svanborg, Apoptosis-like death in bacteria induced by HAMLET, a human milk lipid–protein complex, PLoS One 6 (2011) e17717.
[25] C.R. Brinkmann, S. Theil, D.E. Otzen, Protein–fatty acid complexes: biochemistry, biophysics and function, FEBS J. 280 (2013) 1733–1749.
[26] M.D. Resh, Myristylation and palmitylation of Src family members: the fats of the matter, Cell 76 (1994) 411–413.
[27] M. Mosior, E.S. Golini, R.M. Epand, Chemical specificity and physical properties of the lipid bilayer in the regulation of protein kinase C by anionic phospholipids: evidence for the lack of a specific binding site for phosphatidylserine, Proc. Natl. Acad. Sci. U. S. A. 93 (1996) 1907–1912.
[28] A. Mulgrew-Nesbitt, K. Diraviyam, J. Wang, S. Singh, P. Murray, Z. Li, L. Rogers, N. Mirkovic, D. Murray, The role of electrostatics in protein–membrane interactions, Biochim. Biophys. Acta 1761 (2006) 812–826.
[29] I. Vorobyov, T.W. Allen, On the role of anionic lipids in charged protein interactions with membranes, Biochim. Biophys. Acta 1808 (2011) 1673–1683.
[30] C.B. Baron, V. Coburn, Comparison of two copper reagents for detection of saturated and unsaturated neutral lipids by charring densitometry, J. Liq. Chromatogr. 7 (1984) 2793–2801.
[31] C.W.F. McClare, An accurate and convenient organic phosphorus assay, Anal. Biochem. 39 (1971) 527–530.
[32] G. Le Goff, M.F. Vitha, R.J. Clarke, Orientational polarisability of lipid membrane surfaces, Biochim. Biophys. Acta 1768 (2007) 562–570.
[33] R.P. Haugland, Handbook of Fluorescent Probes and Research Chemicals, 6th ed. Molecular Probes, Eugene, OR, 1996.
[34] M.F.M. Engel, C.P.M. van Mierlo, A.J.W.G. Visser, Kinetic and structural characterization of adsorption-induced unfolding of bovine α-lactalbumin, J. Biol. Chem. 277 (2002) 10922–10930.
[35] R.C. MacDonald, R.I. MacDonald, B.Ph.M. Menco, K. Takeshita, N.K. Subbarao, L.R. Hu, Small-volume extrusion apparatus for preparation of large, unilamellar vesicles, Biochim. Biophys. Acta 1061 (1991) 297–303.
[36] P.M. Matos, T. Freitas, M.A.R.B. Castanho, N.C. Santos, The role of blood cell membrane lipids on the mode of action of HIV-1 fusion inhibitor sifuvirtide, Biochem. Biophys. Res. Commun. 403 (2010) 270–274.
[37] R.J. Clarke, D.J. Kane, Optical detection of membrane dipole potential: avoidance of fluidity and dye-induced effects, Biochim. Biophys. Acta 1323 (1997) 223–239.
[38] S. Haldar, R.K. Kanaparthi, A. Samanta, A. Chattopadhyay, Differential effect of cholesterol and its biosynthetic precursors on membrane dipole potential, Biophys. J. 102 (2012) 1561–1569.
[39] J.R. Lakowicz, Principles of Fluorescence Spectroscopy, 3rd ed. Springer, New York, 2006.

[40] F.S. Abrams, E. London, Extension of the parallax analysis of membrane penetration depth to the polar region of model membranes: use of fluorescence quenching by a spin-label attached to the phospholipid polar headgroup, Biochemistry 32 (1993) 10826–10831.
[41] J.M.H. Kremer, M.W. van der Esker, C. Pathmamanoharan, P.H. Wiersema, Vesicles of variable diameter prepared by a modified injection method, Biochemistry 16 (1977) 3932–3935.
[42] A. Chattopadhyay, S. Mukherjee, R. Rukmini, S.S. Rawat, S. Sudha, Ionization, partitioning, and dynamics of tryptophan octyl ester: implications for membrane-bound tryptophan residues, Biophys. J. 73 (1997) 839–849.
[43] G.C. Chen, J.T. Yang, Two-point calibration of circular dichrometer with d-10-camphorsulfonic acid, Anal. Lett. 10 (1977) 1195–1207.
[44] J. Cladera, P. O'Shea, Intramembrane molecular dipoles affect the membrane insertion and folding of a model amphiphilic peptide, Biophys. J. 74 (1998) 2434–2442.
[45] P.M. Matos, S. Goncalves, N.C. Santos, Interaction of peptides with biomembranes assessed by potential-sensitive fluorescent probes, J. Pept. Sci. 14 (2008) 407–415.
[46] P.M. Matos, M.A.R.B. Castanho, N.C. Santos, HIV-1 fusion inhibitor peptides enfuvirtide and T-1249 interact with erythrocyte and lymphocyte membranes, PLoS One 5 (2010) e9830.
[47] V. Montana, D.L. Farkas, L.M. Loew, Dual-wavelength ratiometric fluorescence measurements of membrane potential, Biochemistry 28 (1989) 4536–4539.
[48] E. Gross, R.S. Bedlack, L.M. Loew, Dual-wavelength ratiometric fluorescence measurement of the membrane dipole potential, Biophys. J. 67 (1994) 208–216.
[49] B.R. Lentz, Membrane "fluidity" as detected by diphenylhexatriene probes, Chem. Phys. Lipids 50 (1989) 171–190.
[50] J.J. Kremer, D.J. Sklansky, R.M. Murphy, Profile of changes in lipid bilayer structure caused by β-amyloid peptide, Biochemistry 40 (2001) 8563–8571.
[51] S. Mukherjee, A. Chattopadhyay, Wavelength-selective fluorescence as a novel tool to study organization and dynamics in complex biological systems, J. Fluoresc. 5 (1995) 237–246.
[52] A. Chattopadhyay, Exploring membrane organization and dynamics by the wavelength-selective fluorescence approach, Chem. Phys. Lipids 122 (2003) 3–17.
[53] H. Raghuraman, D.A. Kelkar, A. Chattopadhyay, Novel insights into protein structure and dynamics utilizing the red edge excitation shift approach, in: C.D. Geddes, J.R. Lakowicz (Eds.), Reviews in Fluorescence 2005, vol. 2, Springer, New York, 2005, pp. 199–224.
[54] A.P. Demchenko, Site-selective red-edge effects, Methods Enzymol. 450 (2008) 59–78.
[55] S. Haldar, A. Chaudhuri, A. Chattopadhyay, Organization and dynamics of membrane probes and proteins utilizing the red edge excitation shift, J. Phys. Chem. B 115 (2011) 5693–5706.
[56] A. Chattopadhyay, S. Haldar, Dynamic insight into protein structure utilizing red edge excitation shift, Acc. Chem. Res. 47 (2014) 12–19.
[57] S.S. Rawat, D.A. Kelkar, A. Chattopadhyay, Monitoring gramicidin conformations in membranes: a fluorescence approach, Biophys. J. 87 (2004) 831–843.
[58] H. Raghuraman, A. Chattopadhyay, Organization and dynamics of melittin in environments of graded hydration: a fluorescence approach, Langmuir 19 (2003) 10332–10341.
[59] S.S. Rawat, S. Mukherjee, A. Chattopadhyay, Micellar organization and dynamics: a wavelength-selective fluorescence approach, J. Phys. Chem. B 101 (1997) 1922–1929.
[60] S.S. Rawat, A. Chattopadhyay, Structural transition in the micellar assembly: a fluorescence study, J. Fluoresc. 9 (1999) 233–244.
[61] H. Raghuraman, S.K. Pradhan, A. Chattopadhyay, Effect of urea on the organization and dynamics of Triton X-100 micelles: a fluorescence approach, J. Phys. Chem. B 108 (2004) 2489–2496.
[62] D.A. Kelkar, A. Chattopadhyay, Depth-dependent solvent relaxation in reverse micelles: a fluorescence approach, J. Phys. Chem. B 108 (2004) 12151–12158.
[63] A.K. Ghosh, R. Rukmini, A. Chattopadhyay, Modulation of tryptophan environment in membrane-bound melittin by negatively charged phospholipids: implications in membrane organization and function, Biochemistry 36 (1997) 14291–14305.
[64] A. Chattopadhyay, E. London, Parallax method for direct measurement of membrane penetration depth utilizing fluorescence quenching by spin-labeled phospholipids, Biochemistry 26 (1987) 39–45.
[65] A. Chattopadhyay, Membrane penetration depth analysis using fluorescence quenching: a critical review, in: B.P. Gaber, K.R.K. Easwaran (Eds.), Biomembrane Structure and Function: The State of the Art, Adenine Press, Schenectady, New York, 1992, pp. 153–163.
[66] E. London, A.S. Ladokhin, Measuring the depth of amino acid residues in membrane-inserted peptides by fluorescence quenching, in: D. Benos, S. Simon (Eds.), Current Topics in Membranes, Elsevier, San Diego, CA, 2002, pp. 89–115.
[67] A. Chattopadhyay, M.G. McNamee, Average membrane penetration depth of tryptophan residues of the nicotinic acetylcholine receptor by the parallax method, Biochemistry 30 (1991) 7159–7164.
[68] R.D. Kaiser, E. London, Location of diphenylhexatriene (DPH) and its derivatives within membranes: comparison of different fluorescence quenching analyses of membrane depth, Biochemistry 37 (1998) 8180–8190.
[69] M.R.R. de Planque, B.B. Bonev, J.A. Demmers, D.V. Greathouse, R.E. Koeppe II, F. Separovic, A. Watts, J.A. Killian, Interfacial anchor properties of tryptophan residues in transmembrane peptides can dominate over hydrophobic matching effects in peptide-lipid interactions, Biochemistry 42 (2003) 5341–5348.
[70] W.M. Yau, W.C. Wimley, K. Gawrisch, S.H. White, The preference of tryptophan for membrane interfaces, Biochemistry 37 (1998) 14713–14717.
[71] J.A. Killian, G. von Heijne, How proteins adapt to a membrane–water interface, Trends Biochem. Sci. 25 (2000) 429–434.
[72] D.A. Kelkar, A. Chattopadhyay, Membrane interfacial localization of aromatic amino acids and membrane protein function, J. Biosci. 31 (2006) 297–302.
[73] R.E. Koeppe II, Concerning tryptophan and protein–bilayer interactions, J. Gen. Physiol. 130 (2007) 223–224.
[74] G. Winkler, S.E. Maxwell, C. Ruemmler, V. Stollar, Newly synthesized dengue-2 virus nonstructural protein NS1 is a soluble protein but becomes partially hydrophobic and membrane-associated after dimerization, Virology 171 (1989) 302–305.
[75] E. London, Diphtheria toxin: membrane interaction and membrane translocation, Biochim. Biophys. Acta 1113 (1992) 25–51.
[76] B. Geny, M.R. Popoff, Bacterial protein toxins and lipids: pore formation or toxin entry into cells, Biol. Cell. 98 (2006) 667–678.
[77] V. Anbazhagan, R.S. Damai, A. Paul, M.J. Swamy, Interaction of the major protein from bovine seminal plasma, PDC-109 with phospholipid membranes and soluble ligands investigated by fluorescence approaches, Biochim. Biophys. Acta 1784 (2008) 891–899.
[78] N. Jain, K. Bhasne, M. Hemaswasthi, S. Mukhopadhyay, Structural and dynamical insights into the membrane-bound α-synuclein, PLoS One 8 (2013) e83752.
[79] M. Eilers, G. Schatz, Protein unfolding and the energetics of protein translocation across biological membranes, Cell 52 (1988) 481–483.
[80] J. Kim, H. Kim, Fusion of phospholipid vesicles induced by α-lactalbumin at acidic pH, Biochemistry 25 (1986) 7867–7874.
[81] G.G. Montich, D. Marsh, Interaction of α-lactalbumin with phosphatidylglycerol. Influence of protein binding on the lipid phase transition and lipid acyl chain mobility, Biochemistry 34 (1995) 13139–13145.
[82] S. Sugai, M. Ikeguchi, Conformational comparison between α-lactalbumin and lysozyme, Adv. Biophys. 30 (1994) 37–84.
[83] J.A. Grobler, M. Wang, A.C.W. Pike, K. Brew, Study by mutagenesis of the roles of two aromatic clusters of α-lactalbumin in aspects of its action in the lactose synthase system, J. Biol. Chem. 269 (1994) 5106–5114.
[84] R. Jaini, P. Kesaraju, J.M. Johnson, C.Z. Altuntas, D. Jane-wit, V.K. Tuohy, An autoimmune-mediated strategy for prophylactic breast cancer vaccination, Nat. Med. 16 (2010) 799–803.